

Thermodynamic properties of a simple, confining model

David Blaschke,^a Craig D. Roberts^b and Sebastian Schmidt^{a,c}

^a*Fachbereich Physik, Universität Rostock, D-18051 Rostock, Germany*

^b*Physics Division, Bldg. 203, Argonne National Laboratory,
Argonne IL 60439-4843, USA*

^c*School of Physics and Astronomy, Raymond and Beverly Sackler Faculty of Exact
Sciences, Tel Aviv University, 69978 Tel Aviv, Israel*

Abstract

We study the equilibrium thermodynamics of a simple, confining, DSE-model of 2-flavour QCD at finite temperature and chemical potential. The model has two phases: one characterised by confinement and dynamical chiral symmetry breaking; and the other by their absence. The phase boundary is defined by the zero of the vacuum-pressure difference between the confined and deconfined phases. Chiral symmetry restoration and deconfinement are coincident with the transition being of first order, except for $\mu = 0$, where it is second order. Nonperturbative modifications of the dressed-quark propagator persist into the deconfined domain and lead to a dispersion law modified by a dynamically-generated, momentum-dependent mass-scale. This entails that the Stefan-Boltzmann limit for the bulk thermodynamic quantities is attained only for large values of temperature and chemical potential.

Key words: Field theory at finite temperature and chemical potential;
Confinement; Dynamical chiral symmetry breaking; Dyson-Schwinger equations

PACS: 11.10.Wx, 12.38.Mh, 12.38.Lg, 24.85.+p

The existence of a “quark-gluon plasma” [QGP] phase of QCD is well established. It is characterised by deconfinement, which means that quarks and gluons have mean free paths that are long in comparison with standard nuclear radii, and the realisation of chiral symmetry in the Wigner mode; i.e., all chiral symmetry breaking effects require an explicit source: the current-quark mass. However, the details of the transition to this phase, and the thermodynamic parameters that characterise it: energy, entropy, pressure, etc.; remain

uncertain. These are the quantities that will determine whether, and under what conditions, the QGP can be engineered in contemporary experiments.

The thermodynamic properties of a theory are completely determined by its partition function [generating functional], and this is the quantity estimated directly in numerical simulations of lattice-QCD actions at finite- T . The Dyson-Schwinger equations [1] [DSEs] provide another nonperturbative means of calculating the partition function: via the evaluation of the Schwinger functions, which are the moments of the measure that defines the partition function. Tractable, quantitative studies of the coupled system of DSEs, examples of which are the QCD gap equation and meson Bethe-Salpeter equation, require a truncation of the tower of integral equations; for example, via a choice for the quark-antiquark scattering kernel. Although it is not possible to judge the fidelity of a particular truncation *a priori*, a systematic approach [2] allows one to address this issue in a direct, practical and constructive manner. The DSEs have been applied extensively at zero temperature and chemical potential to the phenomenology of QCD [3], including the study of strong interaction contributions to weak interaction observables [4].

A robust, qualitative prediction of DSE studies in QCD is that, in the infrared; i.e., for small spacelike- q^2 , the propagation characteristics of the elementary excitations are much altered from that inferred from perturbation theory. For example, the dressed-gluon propagator (2-point function) is strongly enhanced [5], which leads via the QCD gap equation to an infrared enhancement of the light-quark mass-function and, as a result, an infrared suppression of the dressed-light-quark propagator [6]. These modifications are intimately related to confinement and dynamical chiral symmetry breaking and mean that new challenges arise in applying the DSEs to QCD at finite- T and μ [QCD $^\mu_T$]. Therefore, as a precursor to sophisticated DSE analyses of QCD $^\mu_T$, it is useful to explore simple DSE-models in which these features are manifest.

A particularly simple and useful illustrative DSE-model of QCD [7] is specified by a model dressed-gluon propagator that can be generalised to finite- T as [8]

$$g^2 D_{\mu\nu}(\vec{p}, \Omega_k) = \left(\delta_{\mu\nu} - \frac{p_\mu p_\nu}{|\vec{p}|^2 + \Omega_k^2} \right) 2\pi^3 \frac{\eta^2}{T} \delta_{k0} \delta^3(\vec{p}), \quad (1)$$

where $(p_\mu) \equiv (\vec{p}, \Omega_k)$, $\Omega_k = 2k\pi T$ is the boson Matsubara frequency¹ and η is a mass-scale parameter. The infrared enhancement of the dressed-gluon propagator suggested by Refs. [5] is manifest in this model. As an infrared-dominant model that does not represent well the behaviour of $D_{\mu\nu}(\vec{p}, \Omega_k)$ away from $|\vec{p}|^2 + \Omega_k^2 \approx 0$, there are some model-dependent artefacts in our study. However, there is significant merit in its simplicity and, since the artefacts

¹ In our Euclidean formulation $\{\gamma_\mu, \gamma_\nu\} = 2\delta_{\mu\nu}$ with $\gamma_\mu^\dagger = \gamma_\mu$.

are easily identified, the model remains useful as a means of elucidating easily many of the qualitative features of more sophisticated Ansätze.

Using (1) and the “rainbow-approximation”: $\Gamma_\mu^a(k, p) = \frac{1}{2}\lambda^a\gamma_\mu$, for the dressed quark-gluon vertex; the QCD_T^μ gap equation, or DSE for the dressed-quark propagator, is [2]

$$S^{-1}(\vec{p}, \omega_k) = S_0^{-1}(\vec{p}, \omega_k) + \frac{1}{4}\eta^2\gamma_\nu S(\vec{p}, \omega_k)\gamma_\nu, \quad (2)$$

where $S_0^{-1}(\vec{p}, \omega_k) \equiv i\vec{\gamma} \cdot \vec{p} + i\gamma_4(\omega_k + i\mu) + m$, $\omega_k = (2k + 1)\pi T$ is the fermion Matsubara frequency, μ is the chemical potential and m is the current-quark mass. A simplicity inherent in (1) is now apparent: it allows the reduction of an integral equation to an algebraic equation, in whose solution many of the qualitative features of more sophisticated models are manifest, as will become clear. The solution of (2) has the general form

$$S(\tilde{p}_k) = \frac{1}{i\vec{\gamma} \cdot \vec{p}A(\tilde{p}_k) + i\gamma_4(\omega_k + i\mu)C(\tilde{p}_k) + B(\tilde{p}_k)}, \quad (3)$$

where $\tilde{p}_k \equiv (\vec{p}, \omega_k + i\mu)$, and (2) entails that the scalar functions introduced here satisfy

$$\eta^2 m^2 = B^4 + mB^3 + (4\tilde{p}_k^2 - \eta^2 - m^2)B^2 - m(2\eta^2 + m^2 + 4\tilde{p}_k^2)B, \quad (4)$$

$$A(\tilde{p}_k) = C(\tilde{p}_k) = \frac{2B(\tilde{p}_k)}{m + B(\tilde{p}_k)}. \quad (5)$$

Herein we are particularly interested in the chiral limit, $m = 0$. In this case (4) reduces to a quadratic equation for $B(\tilde{p}_k)$, which has two qualitatively distinct solutions. The “Nambu-Goldstone” solution, for which

$$B(\tilde{p}_k) = \begin{cases} \sqrt{\eta^2 - 4\tilde{p}_k^2}, & \Re(\tilde{p}_k^2) < \frac{\eta^2}{4} \\ 0, & \text{otherwise} \end{cases} \quad (6)$$

$$C(\tilde{p}_k) = \begin{cases} 2, & \Re(\tilde{p}_k^2) < \frac{\eta^2}{4} \\ \frac{1}{2} \left(1 + \sqrt{1 + \frac{2\eta^2}{\tilde{p}_k^2}} \right), & \text{otherwise} \end{cases} \quad (7)$$

describes a phase or mode of this model in which: 1) chiral symmetry is dynamically broken, because one has a nonzero quark mass-function, $B(\tilde{p}_k)$, in the absence of a current-quark mass; and 2) the dressed-quarks are confined, because the propagator described by these functions does not have a Lehmann representation. The alternative “Wigner” solution, for which

$$\hat{B}(\tilde{p}_k) \equiv 0 \quad (8)$$

$$\hat{C}(\tilde{p}_k) = \frac{1}{2} \left(1 + \sqrt{1 + \frac{2\eta^2}{\tilde{p}_k^2}} \right), \quad (9)$$

describes a phase of the model in which chiral symmetry is not broken and the dressed-quarks are not confined.

With these two “phases”, characterised by qualitatively different, momentum-dependent modifications of the quark propagator, this DSE-model of QCD_T^μ can be used to explore chiral symmetry restoration and deconfinement, and elucidate aspects of the methodology of such studies.

The pressure is obtained directly from the partition function, \mathcal{Z} , which is the sum of all vacuum-to-vacuum transition amplitudes. In “stationary phase” approximation, the partition function is given by the tree-level auxiliary-field effective action [9] and the pressure is:

$$P[S] \equiv \frac{T}{V} \ln \mathcal{Z} = \frac{T}{V} \left\{ \text{Tr} \text{Ln} [\beta S^{-1}] - \frac{1}{2} \text{Tr} [\Sigma S] \right\}, \quad (10)$$

where $\beta = 1/T$ and the self energy $\Sigma(\tilde{p}_k) \equiv S^{-1}(\tilde{p}_k) - S_0^{-1}(\tilde{p}_k)$. The pressure is a functional of $S(\tilde{p}_k)$. In the absence of interactions $\Sigma \equiv 0$ and (10) yields the free fermion partition function.

We have neglected the gluon contribution to the pressure because, using (1), it is a temperature independent constant. More sophisticated Ansätze do not suffer this defect [8,10], which is associated with the fact that (1) does not represent well the ultraviolet behaviour of $D_{\mu\nu}(k)$ in QCD_T^μ .

The contribution to the partition function of hadrons and hadron-like correlations is also neglected in (10). At the level of approximation consistent with (10) these terms are an additive contribution that can be estimated using the *hadronisation* techniques of Ref. [11]. After a proper normalisation of the partition function; i.e., subtraction of the vacuum contribution, they are the only contributions to the partition function in the domain of confinement. They are easy to calculate and we consider them no further herein.

In studying the phase transition one must consider the relative stability of the confined and deconfined phases, which is measured by the (T, μ) -dependent vacuum pressure difference (or “bag constant” [12])

$$\mathcal{B}(T, \mu) \equiv P[S_{\text{NG}}] - P[S_{\text{W}}], \quad (11)$$

where S_{NG} means (3) obtained from (6) and S_{W} , (3) obtained from (8). $\mathcal{B}(T, \mu) > 0$ indicates the stability of the confined (Nambu-Goldstone) phase

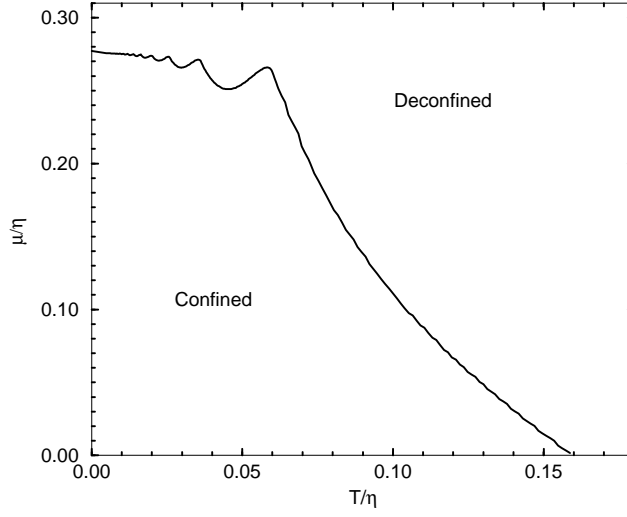


Fig. 1. The phase boundary in the $(\bar{T}, \bar{\mu})$ -plane obtained from (12) and (13); $\eta = 1.06 \text{ GeV}$ [7]. The “structure” in this curve, apparent for small- T , is an artefact of the fact that (1) improperly represents the quark-quark interaction in the ultraviolet.

and hence the phase boundary is specified by that curve in the (T, μ) -plane for which

$$\mathcal{B}(T, \mu) \equiv 0. \quad (12)$$

In the chiral limit, the deconfinement and chiral symmetry restoration transitions in this model are coincident. The critical line is illustrated in Fig. 1, where explicitly

$$\mathcal{B}(T, \mu) = \eta^4 2N_c N_f \frac{\bar{T}}{\pi^2} \sum_{l=0}^{l_{\max}} \int_0^{\bar{\Lambda}_l} dy y^2 \left\{ \Re(2\bar{p}_l^2) - \Re\left(\frac{1}{C(\bar{p}_l)}\right) - \ln |\bar{p}_l^2 C(\bar{p}_l)^2| \right\}, \quad (13)$$

with: $\bar{T} = T/\eta$, $\bar{\mu} = \mu/\eta$; and $\bar{\omega}_{l_{\max}}^2 \leq \frac{1}{4} + \bar{\mu}^2$, $\bar{\Lambda}^2 = \bar{\omega}_{l_{\max}}^2 - \bar{\omega}_l^2$, $\bar{p}_l = (\vec{y}, \bar{\omega}_l + i\bar{\mu})$.

For $\mu = 0$ the transition is second order and the critical temperature is $T_c^0 = 0.159\eta$, which, using the value of $\eta = 1.06 \text{ GeV}$ obtained by fitting the π and ρ masses [7], corresponds to $T_c^0 = 0.170 \text{ GeV}$. This is only 12% larger than the value obtained in Ref. [8] and the order of the transition is the same. However, in the present case the critical exponent is $\beta = 0.5$, which differs from the result $\beta \approx 0.33$ obtained in Ref. [8]. This is an artefact of

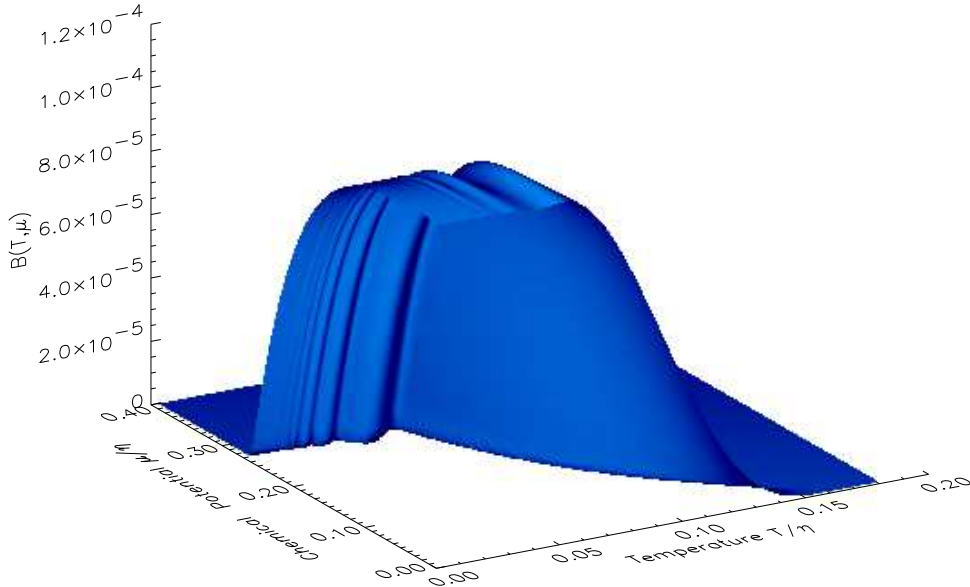


Fig. 2. $\mathcal{B}(T, \mu)$ from (13); $\mathcal{B}(T, \mu) > 0$ marks the confinement domain.

the fact that (1) neglects short-range contributions to the quark-quark interaction and, in particular, it is due to the sharp “cut-off” provided by $B(\tilde{p}_k)$ in (6). Nevertheless, the comparison with Ref. [8] illustrates that this simple model can provide a reasonable guide to the thermodynamic properties of more sophisticated DSE-models of QCD_T^μ .

A feature of the simplicity of the model is that it allows a straightforward analysis of $\mu \neq 0$, where numerical simulations of lattice-QCD actions are not tractable [13], thereby providing valuable insight into deconfinement in this region. For any $\mu \neq 0$ the transition is first-order, as revealed by close scrutiny of Fig. 2. For $T = 0$ the critical chemical potential is $\mu_c^0 = 0.3 \text{ GeV}$. We also see from Fig. 1 that $\mu_c(T)$ is insensitive to T until $T \approx \frac{1}{3} T_c^0$.

The (T, μ) -dependent vacuum pressure difference, $\mathcal{B}(T, \mu)$, is illustrated in Fig. 2. The scale is set by $\mathcal{B}(0, 0) = (0.102 \eta)^4 = (0.109 \text{ GeV})^4$, which can be compared with the value $\sim (0.145 \text{ GeV})^4$ commonly used in bag-like models of hadrons [11]. This pressure is associated with the rearrangement of the confined-quark vacuum; i.e., with the rearrangement of the “ground state”. It does not contribute actively to the thermodynamic pressure, describing only the change in the “stationary point” that defines the auxiliary-field effective-action.

Once in the deconfinement domain, illustrated clearly in Fig. 1, the quarks

contribute an amount

$$P[S_W] = \eta^4 2N_c N_f \frac{\bar{T}}{\pi^2} \sum_{l=0}^{\infty} \int_0^{\infty} dy y^2 \left\{ \ln \left| \beta^2 \tilde{p}_l^2 \hat{C}(\bar{p}_l)^2 \right| - 1 + \Re \left(\frac{1}{\hat{C}(\bar{p}_l)} \right) \right\} \quad (14)$$

to the pressure, which we renormalise to zero on the phase boundary. Just as in the case of free fermions, this expression is formally divergent and one must isolate and define the temperature-dependent, active contribution. This is made difficult by the fact that, in general, $\hat{C}(\bar{p}_l)$ is only known numerically, and hence it is not possible to evaluate $P[S_W]$ analytically. We have developed a method for the numerical evaluation of (14).

Consider the derivative of the integrand in (14):

$$\begin{aligned} \sum_{l=0}^{\infty} \frac{d}{d\bar{T}} \left\{ \ln \left| \beta^2 \tilde{p}_l^2 \hat{C}(\bar{p}_l)^2 \right| - 1 + \Re \left(\frac{1}{\hat{C}(\bar{p}_l)} \right) \right\} = \\ \sum_{l=0}^{\infty} \left\{ -\frac{1}{\bar{T}} \left[\frac{(y - \bar{\mu})^2}{(y - \bar{\mu})^2 + \bar{\omega}_l^2} + \frac{(y + \bar{\mu})^2}{(y + \bar{\mu})^2 + \bar{\omega}_l^2} \right] + \Re \left(\frac{2\hat{C}(\bar{p}_l) - 1}{\hat{C}(\bar{p}_l)^2} \frac{d\hat{C}(\bar{p}_l)}{d\bar{T}} \right) \right\}. \end{aligned} \quad (15)$$

In the absence of interactions $C(\bar{p}_l) \equiv 1$, the second term is zero and

$$-\frac{2}{\bar{T}} \sum_{l=0}^{\infty} \left[\frac{(y - \bar{\mu})^2}{(y - \bar{\mu})^2 + \bar{\omega}_l^2} + \frac{(y + \bar{\mu})^2}{(y + \bar{\mu})^2 + \bar{\omega}_l^2} \right] = \frac{d}{d\bar{T}} \left\{ \frac{e(y)}{\bar{T}} + \mathcal{I}(e(y)) \right\}, \quad (16)$$

where in this case $e(y) = y$ and

$$\mathcal{I}(\zeta) = \ln \left[1 + \exp \left(-\frac{\zeta - \bar{\mu}}{\bar{T}} \right) \right] + \ln \left[1 + \exp \left(-\frac{\zeta + \bar{\mu}}{\bar{T}} \right) \right]. \quad (17)$$

Appropriately inserting (16) for the parenthesised term in (14), and neglecting T -independent terms one obtains,

$$P[S_0] = \eta^4 N_c N_f \frac{\bar{T}}{\pi^2} \int_0^{\infty} dy y^2 \mathcal{I}(y) \quad (18)$$

$$= \eta^4 N_c N_f \frac{1}{12\pi^2} \left(\bar{\mu}^4 + 2\pi^2 \bar{\mu}^2 \bar{T}^2 + \frac{7}{15} \pi^4 \bar{T}^4 \right), \quad (19)$$

which is the massless, free particle pressure.

To proceed we assume that the nontrivial momentum dependence of $\hat{C}(\bar{p}_l)$, which is manifest in all DSE-models of QCD, acts primarily to modify the

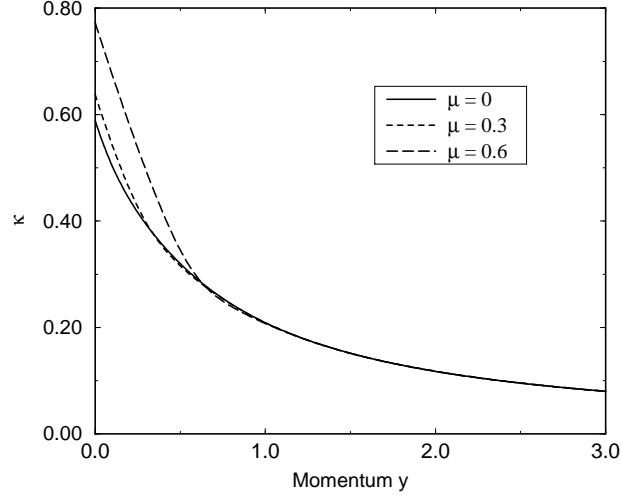


Fig. 3. $\kappa(y, \bar{\mu})$, which describes the nonperturbative modification of the free particle dispersion law, for $\bar{\mu} = 0, 0.3, 0.6$. By assumption, it is independent of T .

usual massless, free particle dispersion law. We evaluate numerically the sum on the right-hand-side of (15) and use the form on the right-hand-side of (16) to fit a modified, T -independent dispersion law, $\underline{e}(y, \bar{\mu}) = y + \kappa(y, \bar{\mu})$, to the numerical results. The existence of a $\kappa(y, \bar{\mu})$ that provides a good χ^2 -fit on the deconfinement domain is understood as an *a posteriori* justification of this assumption. In our calculations, on the entire T -domain, the relative error between the fit and the numerical results is $< 10\%$.

We illustrate the calculated form of $\kappa(y, \bar{\mu})$ in Fig. 3; it only depends weakly on $\bar{\mu}$. The form indicates that the result of the persistence of nonperturbative effects into the domain of deconfinement; i.e., the nontrivial momentum dependence of $\hat{C}(\bar{p}_l)$ and its slow evolution to the asymptotic value $\hat{C}(\bar{p}_l) = 1$, is to generate a mass-scale in the massless dispersion law: $\kappa(0, 0) \simeq 0.6 \sim 2\bar{\mu}_c^0$. This mass-scale is unrelated to the chiral-symmetry order parameter, $B(\vec{0}, \omega_0 + i\mu)$, and is a qualitatively new feature of this study. For $\bar{\mu} > 5\bar{\mu}_c^0$ the explicit mass-scale introduced by the chemical potential overwhelms this dynamically generated scale.

With this result (14) becomes

$$P[S_W] = \eta^4 N_c N_f \frac{\bar{T}}{\pi^2} \int_0^\infty dy y^2 \mathcal{I}(\underline{e}(y, \bar{\mu})), \quad (20)$$

and the quark pressure in this DSE-model of QCD_T^μ is

$$P_q(T, \mu) = \theta(\mathcal{D}) \{P[S_W] - P[S_W]|_{\partial\mathcal{D}}\} \quad (21)$$

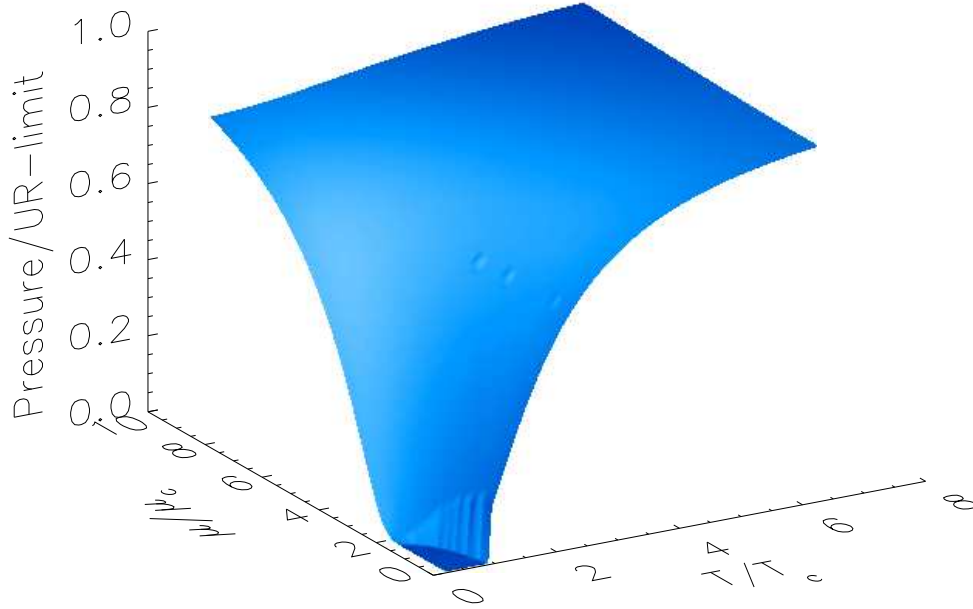


Fig. 4. The quark pressure, $P_q(\bar{T}, \bar{\mu})$, normalised to the free, massless (or Ultra-Relativistic) result, (19).

where \mathcal{D} is the domain marked “Deconfined” in Fig. 1, $\theta(\mathcal{D})$ is a step function, equal to one for $(T, \mu) \in \mathcal{D}$, and $P[S_W]|_{\partial\mathcal{D}}$ indicates the evaluation of this expression on the boundary of \mathcal{D} , as defined by the intersection of a straight-line from the origin in the (T, μ) -plane to the argument-value. It is plotted in Fig. 4, which illustrates clearly that in this model the free particle (Stefan-Boltzmann) limit is reached at large values of \bar{T} and $\bar{\mu}$. The approach to this limit is slow, however. For example, at $\bar{T} \sim 0.3 \sim 2\bar{T}_c^0$, or $\bar{\mu} \sim 1.0 \sim 3\bar{\mu}_c^0$, (21) is only $\frac{1}{2}$ of the free particle pressure, (19). A qualitatively similar result is observed in numerical simulations of lattice-QCD actions at finite- T [14]. This feature results from the slow approach to zero with y of $\kappa(y, \bar{\mu})$, illustrated in Fig. 3, and emphasises the persistence of the momentum dependent modifications of the quark propagator.

With the definition and calculation of the pressure, $P_q(T, \mu)$, or equivalently the partition function, all of the remaining bulk thermodynamic quantities that characterise our DSE-model of QCD_T^μ can be calculated. As an example, in Fig. 5 we plot the “interaction measure”: $\Delta \equiv \epsilon - 3P$, where ϵ is the energy density. This is zero for an ideal gas, hence the nomenclature: Δ measures the interaction-induced deviation from ideal gas behaviour. This figure provides a very clear indication of the persistence of nonperturbative effects into the deconfinement domain.

We have explored the equilibrium thermodynamics of a simple, confining, DSE-model of QCD_T^μ , defined by the model dressed-gluon propagator in (1),

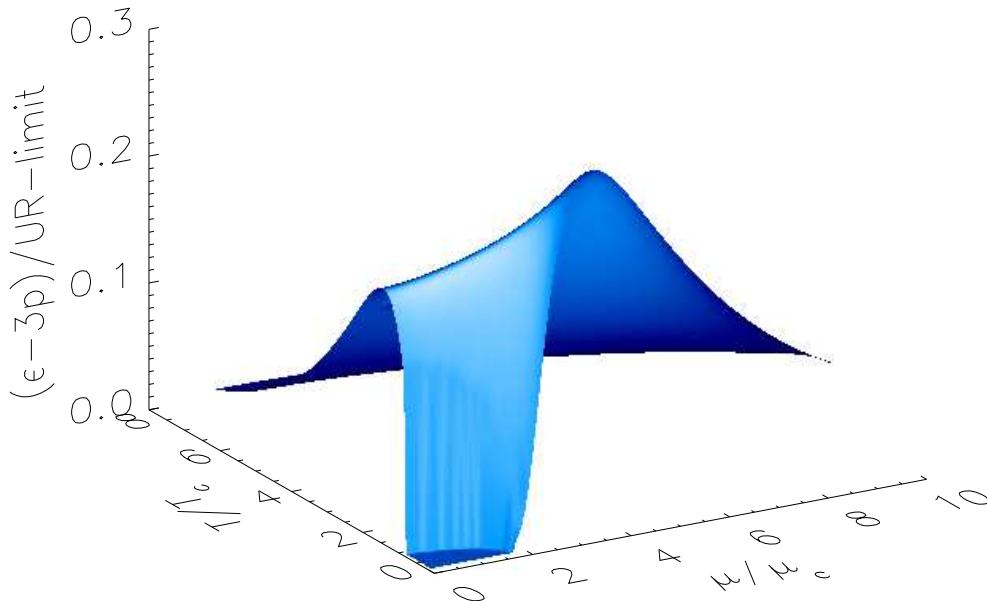


Fig. 5. The “interaction measure”, $\Delta(T, \mu)$, normalised to the free, massless result for the pressure, (19).

which shares many of the features found in DSE-models with more realistic Ansätze for the dressed-gluon propagator [8]. The simplicity of the model allows a straightforward analysis of the bulk thermodynamics for finite chemical potential as well as finite temperature.

Deconfinement and chiral symmetry restoration are coincident and the phase boundary, defined by that curve in the (T, μ) -plane for which the temperature- and chemical-potential-dependent “bag constant”, (13), vanishes, is illustrated in Fig. 1. The transition is first order except for $\mu = 0$. We expect these results to be qualitatively reliable; a more sophisticated model leads only to a slight reduction in the $\mu = 0$ critical temperature [8] and an increase in the $T = 0$ critical chemical potential [10].

The quark pressure is given by (21) and is illustrated in Fig. 4. It is zero in the confining domain and approaches the Stefan-Boltzmann limit for a massless, free particle only for relatively large values of T and μ . The calculation of the pressure is complicated by the momentum dependence of the nonperturbatively-dressed quark propagator. This generates a nonperturbative mass-scale in the dispersion relation for the deconfined quark, Fig. 3. It is an essential feature of this study and is responsible for the slow attainment of the Stefan-Boltzmann limit.

The persistence of nonperturbative effects into the deconfining domain is elucidated in the “interaction measure”, which is illustrated as a function of T

and μ in Fig. 5. The slow attainment of the Stefan-Boltzmann limit at finite- T observed in lattice simulations of QCD_T^μ is mirrored in a slow approach to this limit with increasing μ .

We acknowledge useful conversations with A. Höll and P. Maris. DB and SS gratefully acknowledge the hospitality of the Physics Division at ANL; and CDR that of the Max-Planck-Group and the Department of Physics at the University of Rostock. CDR acknowledges a stipend from the Max-Planck-Gesellschaft; and SS, financial support from the MINERVA Foundation. This work was supported in part by the Deutscher Akademischer Austauschdienst; by the Department of Energy, Nuclear Physics Division, under contract no. W-31-109-ENG-38; by the National Science Foundation under grant no. INT-9603385; and benefited from the resources of the National Energy Research Scientific Computing Center.

References

- [1] C. D. Roberts and A. G. Williams, *Prog. Part. Nucl. Phys.* **33** (1994) 477.
- [2] A. Bender, C. D. Roberts and L. v. Smekal, *Phys. Lett. B* **380** (1996) 7.
- [3] P. C. Tandy, “Hadron physics from the Global Colour Model of QCD”, archive: nucl-th/9705018, to appear in *Prog. Part. Nucl. Phys.* **39** (1997); M. A. Pichowsky and T.-S. H. Lee, “Exclusive diffractive processes and the quark substructure of mesons”, archive: nucl-th/9612049, to appear in *Phys. Rev. D*.
- [4] Yu. L. Kalinovsky, K. L. Mitchell and C. D. Roberts, *Phys. Lett. B* **399** (1997) 22; M. B. Hecht and B. H. J. McKellar, “Dipole Moments of the Rho Meson”, archive: hep-ph/9704326.
- [5] M. Baker, J. S. Ball and F. Zachariasen, *Nucl. Phys. B* **186** (1981) 531; *ibid.*, 560; D. Atkinson, *et al.*, *Nuovo Cimento A* **77** (1983) 197; N. Brown and M. R. Pennington, *Phys. Rev. D* **39** (1989) 2723.
- [6] A. G. Williams, G. Krein and C. D. Roberts, *Ann. Phys.* **210** (1991) 464; H. J. Munczek and P. Jain, *Phys. Rev. D* **46** (1992) 438.
- [7] H. J. Munczek and A. M. Nemirovsky, *Phys. Rev. D* **28** (1983) 181.
- [8] A. Bender, *et al.*, *Phys. Rev. Lett.* **77** (1996) 3724.
- [9] R. W. Haymaker, *Riv. Nuovo Cim.* **14**, series 3, no. 8 (1991).
- [10] G. Poulis, C. D. Roberts and A. W. Thomas, in progress.
- [11] R. T. Cahill, *Aust. J. Phys.* **42** (1989) 171.
- [12] R. T. Cahill and C. D. Roberts, *Phys. Rev. D* **32** (1985) 2419.

- [13] M.-P. Lombardo, J. B. Kogut and D. K. Sinclair, Phys. Rev. D **54** (1996) 2303.
- [14] J. Engels, *et al.*, Phys. Lett. B **396** (1997) 210.